# SPATIALLY RESOLVED SURFACE ACOUSTIC WAVE STUDIES FOR IMAGE PROCESSING AND CHEMICAL SENSORS

A. C. Mueller, H.-J. Kutschera, and A. Wixforth
Center for Nanoscience, University of Munich, D-80539 Munich, Germany

**Abstract — The interaction between a surface acoustic wave (SAW) and photo-generated charge carriers in a piezoelectric semiconductor substrate leads to pronounced changes in the transmission properties of the SAW. Depending on the charge carrier density one observes a wave attenuation and a change in sound velocity in the SAW delay line. Using specially designed surface acoustic wave transducers, we are able to spatially resolve this interaction. The transducers used for this purpose consist of fan shaped interdigated metal fingers, which show a broadband frequency transmission. It turns out, that for such transducers the excited SAW propagates on a narrow path, whose position can be controlled by the driving frequency. If the SAW propagates along a path where defined molecules from the environment are adsorbed, the SAW transmission properties are also changed. This can be used for the chemical sensors.**

Keywords — SAW, SAW-camera, chemical sensor, image processing

## 1. INTRODUCTION

Sophisticated surface acoustic wave (SAW) device technology together with well defined electronic properties of a semiconductor leads to very interesting applications of optical signal processing.
In a piezoelectric crystal the SAW is accompanied by electric fields due to crystal deformations. The coupling is summarized in the electromechanical coupling constant $K^2_{eff}$. For a conducting sheet close to the surface having a conductivity $\sigma$ the change of the SAW velocity is given by [1]

$$\frac{\Delta v}{v} = \frac{K^2_{eff}}{2} \frac{1}{1+(\sigma/\sigma_m)^2}, \qquad (1)$$

where $\sigma_m$ denotes the critical sheet conductivity. The largest energy transfer from the SAW to the charge carrier system occurs at $\sigma = \sigma_m$. Mobile charge carriers move in the electric field generated by the SAW and dissipate energy because of finite resistance. This energy loss leads to an attenuation $\Gamma$ of the acoustic wave's amplitude:

$$\Gamma = \frac{K^2_{eff}}{2} k_{SAW} \frac{\sigma/\sigma_m}{1+(\sigma/\sigma_m)^2}. \qquad (2)$$

In a hybrid system consisting of a submicron thick semiconducting AlGaAs/InGaAs-heterostructure on top of a strong piezoelectric substrate, like e.g. $LiNbO_3$, attenuations of about 20 dB and phase shifts of several hundred degrees have been demonstrated [2]. Therefore, SAW measurements are a very sensitive tool to determine fundamental properties of semiconductors and have been used to investigate e.g. two-dimensional electron systems in the quantum hall regime and the fractional quantum hall regime [3, 4].

Another very important application of SAW devices are chemical sensors. With different chemical or biological functionalized surfaces these devices are very sensitive to well specified substances. The SAW is then either sensitive on the additional mass loading [5] or on the additional charge carriers excited by chemical reactions [6] on the substrate surface. Usually the additional mass on the SAW device can be measured by a frequency shift $\Delta f$ of a SAW resonator [7, 8]. Because of our interdigital transducer design we do not use an oscillator circuit. Instead we are measuring the mass induced phase shift in the SAW signal and hence the change in SAW velocity. The dependency of the velocity shift on additional mass is given by:

$$\frac{\Delta v}{v_0} \propto \rho_s f_0. \qquad (3)$$

where $f_0$ is the fundamental device frequency and $\rho_s$ is the area density of mass.

## 2. TAPERED INTERDIGITAL TRANSDUCER

To achieve spatial resolution we use so called fan shaped interdigital transducers, first introduced by Van de Heuvel [9]. In this special design of IDT the finger period is decreased monotonously along the aperture $L$, described by the tapering factor $p$ [10]. This decrease causes a broadening of the transmission signal. The resulting transmission signal is a bandpass. For a frequency within such a bandpass the IDT matches the resonance only in a confined part of the aperture and launches a SAW on a very narrow path (see fig. 1). In addition, we

E-mail: alexander.mueller@physik.uni-muenchen.de

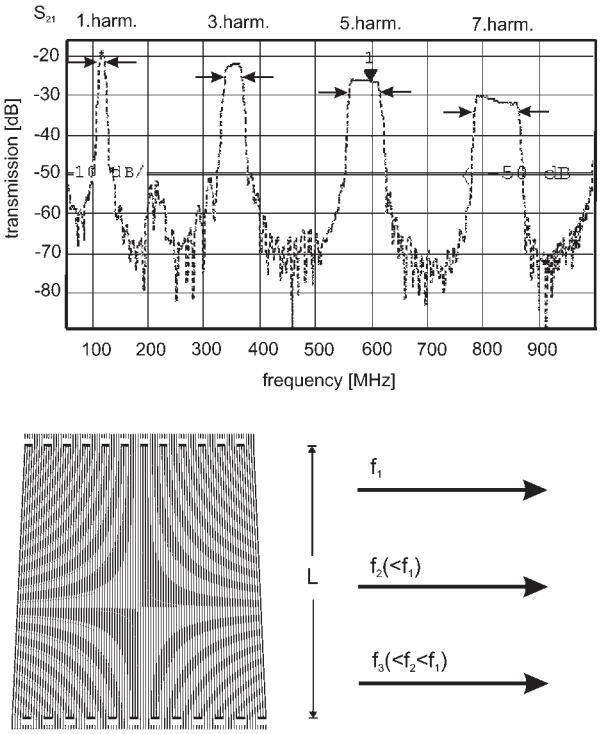


Fig. 1. Upper part: Transmission signal $S_{21}$ of a delay line with fan shaped split 4 IDTs . Maximum transmission occurs at the odd harmonics of the IDT periodicity. Here, we show the odd harmonics from the 1st to the 7th. The IDTs with 12 finger pairs are shown in the lower part of this figure. The taper factor is 10%.

can use multiple split fingers which reduce internal reflections and give us the opportunity to work with different frequencies using one single delay line. These frequencies are odd harmonics of the resonant ground frequency. The value $\frac{\text{bandpass}}{\text{middle frequency}}$ is approximately the tapering factor p which represents a constant value. Therefore the bandpass spreads with higher frequencies for a constant tapering factor. A typical transmission signal of this design is shown in fig. 1.

The width of the SAW path limits the spatial resolution. It was already shown that the width decreases with increasing taper factor before it reaches a minimum and then increases again due to diffraction [11]. Diffraction gains in importance, if the confinement reaches the order of the wavelength. Sauer et al. have been able to directly demonstrate diffraction for GaAs by X-ray imaging [12]. For small tapering factors one can neglect diffraction and estimate the SAW path's width like the following:

$$width_{SAW} = \frac{bandwidth_{normalIDT}}{bandpass_{fanshapedIDT}} \cdot L. \quad (4)$$

The transmitted 3dB bandwidth of a non fan shaped IDT is almost constant for all odd harmonics and is for our design about 6 MHz. Therefore the estimated SAW path for the 5th harmonic is around 45 µm.

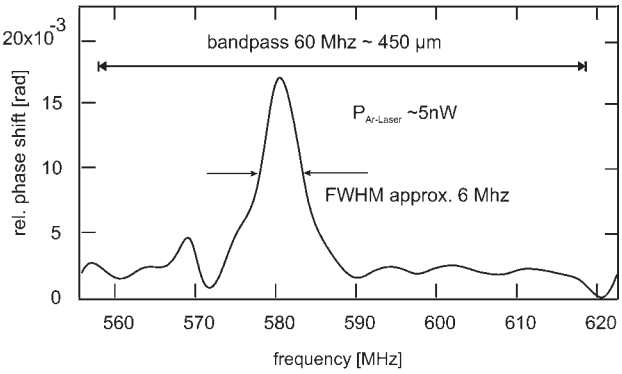


Fig. 2. The spatial resolution in one dimension of an optically generated local electron-hole-plasma with fan shaped interdigital transducers

To enhance spatial resolution a taper factor of 20 % was tested. The transmitted signal is about 15 dB less than for a taper factor of 10 % on $LiNbO_3$ 128°-cut which is according with what we expected. The spatial resolution, measured with a thin needle placed on the delay line to damp the SAW intensity showed still good results.

As substrate we use either $LiNbO_3$ 128°-cut or GaAs(001). In the case of GaAs(001) the symmetries along the x and y axis are equivalent. Therefore the transmission signals of perpendicular SAW delay lines are the same. The $LiNbO_3$ 128°-cut has different symmetries in x-direction and the perpendicular ỹ-direction. For our delay line layout the transmission in ỹ-direction is about 10 dB lower.

## 3. SPATIALLY RESOLVED OPTICAL MEASUREMENTS

In a semiconducting substrate illuminated by a laser, charge carriers are generated, if the photon energy of the laser is larger than the energy gap between valence and conductance band. The number of photogenerated charge carriers is proportional to the laser intensity, which is in turn proportional to the conductivity $\sigma$. The illumination induced change in conductivity alters the soundvelocity and the SAW amplitude according to equations (1) and (2) respectively.

The spatial resolved change in the phase signal due to illumination with an Argon laser ($\lambda$=488 nm) and a spot diameter of about 5 µm is plotted in fig. 2. The FWHM of the measured phase shift is 6 MHz, which corresponds to 45 µm for the given transducer geometry. The difference between the measured and the real spot size is due to the finite width of the SAW path (as shown in section 1.). Within the range of laser intensities we used, we believe that the re-

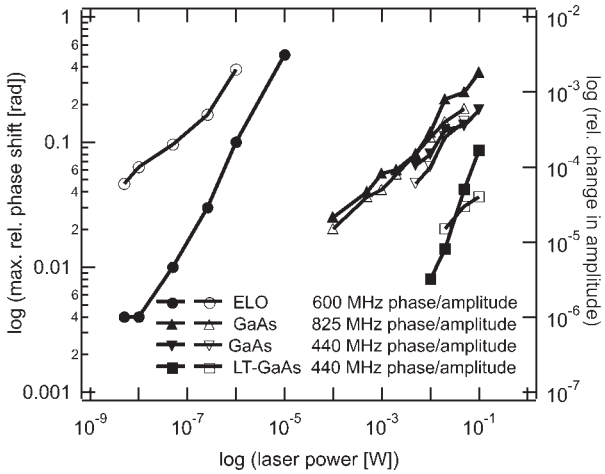


Fig. 3. Dependence of maximum change in phase and amplitude of the SAW signal to different laser intensities. The diameter of the laser spot at the surface is about 5$\mu$m.

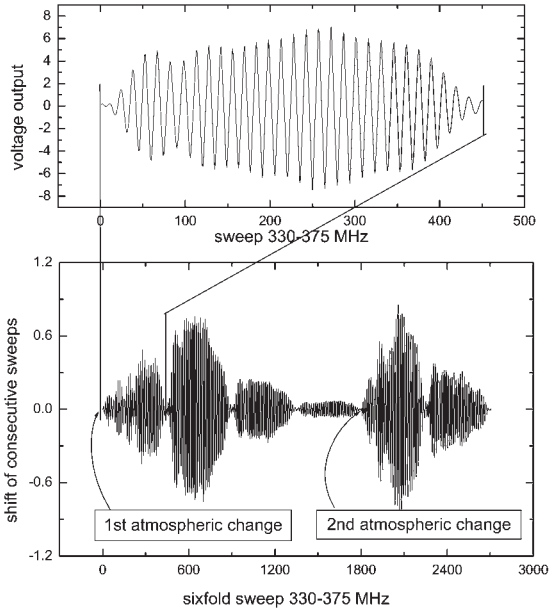


Fig. 4. Upper part: Mixer signal between DUT and reference signal leads after low pass to $\cos\Delta\varphi$ where $\Delta\varphi$ is the phase difference of the mixer input signals. Lower part shows the differences $\cos\Delta\varphi_1 - \cos\Delta\varphi_2$ of consecutive sweeps.

sulting sheet conductivity $\sigma$ is always below the critical sheet conductivity $\sigma_m(\mathrm{GaAs}) = 3.3 \cdot 10^{-7}\Omega^{-1}$.

The relative change in phase and amplitude of the transmitted SAW signal changes with different material properties and different driving frequencies of the device. In this work we present three different GaAs devices. The first one is pure GaAs, which is characterized at the two different driving frequencies 440 and 825 MHz. With increasing frequency more oscillations fit into the interacting area and hence the sensitivity of the device increases (compare triangled symbols in fig. 3). In GaAs grown at low temperatures (LT-GaAs) the mobility of electrons is lower ($\mu_e$ in the order of $10^2\mathrm{cm}^2/\mathrm{V{\cdot}s$) as compared to the electron mobility in GaAs grown at higher temperatures ($\mu_e = 8{\cdot}10^3\mathrm{cm}^2/\mathrm{V{\cdot}s$). To reach the same sheet conductivity $\sigma = en_e\mu_e$, where $e$ is the elementary charge, one has to increase the two dimensional electron density $n_e$ and consequently generate more charge carriers. This is shown in fig. 3 squared data symbols.

It turned out, that a very sensitive tool to detect very small laser intensity is a submicron thick epitaxial lift-off GaAs layer adhering via van der Waals forces on a $LiNbO_3$ surface. The electromechanical coefficient $K^2_{eff,\mathrm{LiNbO_3}}$ is 2 orders of magnitude larger than for GaAs and in addition charge carriers are restricted close to the surface, since they cannot escape the GaAs layer. Therefore the charge carriers are located at highest electric fields.

## 4. CHEMICAL SENSORS

The principle of spatially resolved measurements of an optical generated charge carrier distribution on the substrate surface is also applicable to measure atmospheric changes. Up to now, different setups were tested to optimize the system for further experiments. Commercial chemical sensors, based on SAW devices, consist of two delay lines. One of them is functionalized and sensitive to adsorbants and the other one serves as a reference [5].

In our experiments, we use only one delay line with fan shaped interdigital transducers as sensor device and take the generator as a reference. The device and the reference signal are mixed and sent through a low pass filter. The resulting signal is the cosine of the phase difference between the two input signals $\cos\Delta\varphi$ (Upper graph of fig. 4). Up to now our device was not structured with functionalized layers on the delay line. Nevertheless, the device was tested under ambient air with and without additional humidity. One frequency sweep (0.1 MHz step size) between 330 and 375 MHz took about 6 minutes. The timescale on which changes can be resolved is limited by the duration of one sweep. The limit for spatial resolution is given by the width of the SAW path.

## 5. CONCLUSION

With fan shaped interdigital transducers we are able to spatially resolve a small laser spot on the device surface in two dimensions. We investigated several material systems and achieved sensitivity over 7 orders of magnitude in the laser intensity from $2.5 \cdot 10^{-2}$ to $5 \cdot 10^5\,\mathrm{W/cm}^2$. It turns out that a semiconductor piezoelectric hybrid structure consisting

of a submicron thick GaAs layer on top of a $LiNbO_3$ crystal is a very sensitive tool to detect small light intensities due to the large coupling coefficient $K^2_{eff}$ in this system. The adequate substrate to spatially resolve large laser intensities is GaAs grown at low temperatures. In this material the defect concentration is bigger and therefore the charge carrier mobility is lower than in GaAs grown at higher temperatures.

Surface acoustic wave devices based on $LiNbO_3$ technology and normal IDTs have been already used to detect changes in ambient conditions. These devices work with normal IDTs. We showed that changes can also be detected with the fan shaped IDTs. To realize a very small and compact artificial nose we plan to structure the delay line with different functionalized, narrow stripes aligned with the SAW's direction of propagation.

## ACKNOWLEDGMENT

This work has been sponsored in part by Advalytix AG, Brunnthal, Germany, and in part by the Bayerische Forschungsstiftung. Fruitful discussions with Prof. J.P. Kotthaus, Prof. Th. Bein, Dr. J. Sauer, and S. Manus (all University of Munich) are gratefully acknowledged.

## References

[1] A. Wixforth, J.P. Kotthaus, and G. Weimann, *Quantum Oscillations in Surface-Acoustic-Wave Attenuation Caused by a Two-Dimensional Electronic System*, Phys. Rev. Lett. **56**, 2104 (1986).

[2] M. Rotter, A.V. Kalameitsev, A.O. Govorov, W. Ruile, and A. Wixforth, *Charge Conveyance and Nonlinear Acoustoelectric Phenomena for Intense Surface Acoustic Waves on a Semiconductor Quantum Well*, Phys. Rev. Lett. **82**, 2171 (1999).

[3] A. Wixforth, J. Scriba, M. Wassermeier, J.P. Kotthaus, G. Weimann, and W. Schlapp, *Surface acoustic waves on* $GaAs/Al_xGa_{1-x}As$ *heterostructures*, Phys. Rev. B. **40**, 7874 (1989).

[4] R.L. Willet, R.R. Ruel, W. West, and L.N. Pfeiffer, *Experimental demonstration of a Fermi surface at one-half filling of the lowest Landau level* Phys. Rev. Lett. **71**, 3846 (1993).

[5] H. Wohltjen, and R. Dessy, *Surface Acoustic Wave Probe for Chemical Analysis*, Anal. Chem. **51**, 1458 (1979).

[6] A. D'Amico, A. Palma, and E. Verona, *Palladium-surface acoustic wave interaction for hydrogen detection*, Appl. Phys. Lett. **41**, 300 (1982).

[7] D. Ballantine, and H. Wohltjen, *Surface Acoustic Wave Device for Chemical Analysis*, Anal. Chem. **61**, 704A (1989).

[8] D. Ballantine, R.M. White, S.J. Martin, A.J. Ricco, E.T. Zellers, G.C. Frye, and H. Wohltjen, *Acoustic Wave Sensors*, Academic Press (1997) ISBN 0-12-077460-7.

[9] A.P. Van de Heuvel, *Use of rotated electrodes for amplitude weighting in interdigital surface wave transducers*, Appl. Phys. Lett. **21**, 280 (1972).

[10] M. Streibl, F. Beil, A. Wixforth, C. Kadow, and A.C. Gossard, *SAW Tomography - Spatially Resolved Charge Detection by SAW in Semiconductor Structures for Imaging Applications*, IEEE Ultrasonic Symposium 1999, p.11.

[11] M. Streibl, H.-J. Kutschera, W. Sauer, and A. Wixforth *Numerical and Experimental Analysis of Complex Surface Acoustic Wave Fields*, IEEE Ultrasonic Symposium 2000.

[12] W. Sauer, M. Streibl, T.H. Metzger, A.G.C. Haubrich, S. Manus, A. Wixforth J. Peisl, A. Mazuelas, J. Hrtwig, and J. Baruchel, *X-ray imaging and diffraction from surface phonons on GaAs*, Appl. Phys. Lett. **75**, 1709 (1999).